

Emerging SYK physics and Wigner-Dyson distribution in polaron system

Chen-Huan Wu *

College of Physics and Electronic Engineering, Northwest Normal University, Lanzhou 730070, China

August 25, 2022

We study the of SYK interactions and Wigner-Dyson distribution in the polaron system through the theoretical study and numerical simulation. The polaron as a long-lived quasiparticle which can be found in the incompressible state has slow momenta and current relaxation in Fermi liquid phase. We reveal the relation between UV cutoff of polaronic momentum Λ_q and its SYK behavior. The SYK behavior of a polaron system, as well as the relation between scattering momentum and the related statistical behaviors has rarely been investigated before. We found that the inversed momentum cutoff Λ_q^{-1} , which plays the role of an essential degree-of-freedom (DOF) other than the fermions, relates to the distribution and statistical variance of polaronic coupling term. By projecting to a 2d square lattice, we consider this problem in position space where the DOF of polaron scattering momenta is replaced by another flavor (denoted as η_Δ with flavor number of order of $O(M)$) which is determined by the site potential difference Δ as well as the site index, and we also applying the self-attention method to searching for the more efficient route to exploiting the many-body behaviors. The algorithm designed by us allow the automatical optimization and prediction for the resulting spectrum to arbitrary accuracy. Although here η_Δ (or Λ_q in terms of the momentum space representation) should be a Gaussian variable with zero mean by its own (noninteracting), but it becomes a Chi-square variable when it couples with the fermionic DOF ($O(N)$). The resulting system follows the statistic of between Gaussian symplectic ensemble (GSE) and Gaussian unitary ensemble (GUE) as long as $O(M) \sim O(N^2/4)$. While in terms of the momentum space representation, different magnitude of Λ_q^{-1} support to different phases, including non-Fermi liquid phase and (disordered) Fermi liquid phase, which correspond to ill-defined and well-defined polarons, respectively, and the suppression to the Gaussian distribution in non-fermi liquid phase by the pairing condensation-induced local coupling of is also being mentioned.

1 Introduction

We consider a two-dimensional $N(N - 1)$ square lattice consist of the fermion index i and j ($i, j = 1, \dots, N$). As we know that to realizing the polaron physics, it requires localization on the momentum space of interacting fermions which leads to vanishingly small scattering momenta $q \rightarrow 0$. Then the polarons which play the role of quasiparticles here can be considered in quasi-one-dimensional system in such a 2d lattice by virtue of the chiral character, and we only consider the polarons contributed by the right-direction effects (a combination effect of

*chenhuanwu1@gmail.com

fermion indices difference and on-site potential difference) on each quasi-one-dimensional chain. By considering the vector potential, the random motion of fermions in opposite directions will cancel each other and leads to zero expectation of polaron feature in each quasi-one-dimensional chains. However, by adding another degree-of-freedom (DOF) which is the randomly distributed on-site potential, the nonzero expectation of polaron feature can be generated. All the on-site potential differences in horizontal direction in this 2d system can be regarded as a Gaussian variable which satisfy $\overline{\Delta_{\alpha\beta}} = 0$, and its variance is close to (but lower than) the typical value $\overline{\Delta_{\alpha\beta}^2} = N^2/4$, where we denote the potential difference on each horizontal lines as $\Delta_{\alpha\beta}$ ($\alpha, \beta = 1, \dots, N$). Although $\Delta_{\alpha\beta}$ is a Gaussian variable by its own, it changes to a Chi-square variable (product of two Gaussian ones) with nonzero mean when it couple with the fermionic DOF. We consider that, for each part of fermion indices (i, j), the probabilities for them to occupy each part of (α, β) are dominated by the rule that the probabilities for each distinct value of $\eta_{\Delta} = |\Delta_{\alpha\beta}|\alpha$ must be the same, which means only the quantity $|\Delta_{\alpha\beta}|\alpha$ (on-site potential difference times the site-index on the left, due to the chiral character of quasi-1d system and vector potential) can be regarded as an independent disorder or DOF relative to fermion DOF, i.e., each part of (i, j) , instead of the $\Delta_{\alpha\beta}$. And the key condition for the realization of polaron behavior the nonzero net potential difference $\Delta_{\alpha,\beta}$, as well as the Wigner-Dyson distribution which should be beyond the GUE region (with character level spacing ratio $\langle r \rangle_{GUE} = 0.59 \sim 0.60$), which implies the thermalization and Gaussian randomness on the on-site potential difference DOF. The Hamiltonian describing the effect of polaron reads

$$H = \sum_{ij;\alpha,\beta} = w_{ij}[\Delta_{\alpha\beta}]c_i^\dagger c_j, \quad (1)$$

where the potential difference $\Delta_{\alpha\beta}$ is the weighted Gaussian variable, and it couples with the fermionic DOF represented by the fermionic indices (i, j). The weighting function w_{ij} depends on the fermion DOF by the requirement that the probability $p_{\eta_{\Delta}}$ must be a constant during the selection by the fermion indices. We summarize our main result [here](#). As long as the system is under this condition, we found that the variance satisfies $\sigma_q^2 = \overline{\Delta_{\alpha\beta}^2} \sim N^2/4$ and the level spacing ratio $\langle r \rangle$ will be of the region between GUE and GSE. The value of this variance is also the size of M (i.e., flavor number of distinct values of $|\Delta_{\alpha\beta}|\alpha$). We also provide another version of the this model in terms of the momentum space representation in Appendix.

2 Gaussian-based self-attention

Projection to this 2d lattice model available us to using the transformer method base on (multi-head) self-attention model to solve this problem. Firstly, we consider the case in the absence of Gaussian weighting term, i.e., considering the unbiased potential difference DOF $\Delta_{\alpha,\beta}$ ($\alpha, \beta = 1, \dots, N$), the self-attention layer reads

$$\mathbf{H} = \text{Attn}(\mathbf{Q}, \mathbf{K}, \mathbf{V}) = \text{Softmax}\left[\frac{\mathbf{Q}\mathbf{K}^T}{\sqrt{\sigma_q^2}}\right]\mathbf{V}, \quad (2)$$

where $\mathbf{Q} = \mathbf{X}\mathbf{W}^{\mathbf{Q}}$, $\mathbf{K} = \mathbf{X}\mathbf{W}^{\mathbf{K}}$, $\mathbf{V} = \mathbf{X}\mathbf{W}^{\mathbf{V}}$, are the query, key, and value matrices, which are all $N \times (N - 1)$ type. \mathbf{X} is the input (α, β) sequence. It is direct to know that when the potential difference DOF is unweighted (or selected) by the fermionic DOF, it behaves as a Gaussian variable, and the probabilities for $\Delta_{ij} = 1, \dots, (N - 1)(i \neq j)$ are unequal, as shown in the simulator-obtained spectrum in Fig.1(a,b), lower value of Δ_{ij} has bigger weight. In this case the net potential difference is zero and the variance is $\overline{\Delta_{ij}^2} \sim N^2/8$, and the level spacing distribution follows the GUE with $\langle r \rangle = 0.59 \sim 0.60$.

2.1 Gaussian-based self-attention

To see the result when the M -DOF couples with the fermionic DOF, we firstly simulate the real case according to the calculated exact probabilities for each part of (α, β) according to the selection rule of fermions, $\partial_{\alpha, \beta} \eta_{\Delta} = 0$, i.e., each value of η_{Δ} has the same weight in the final $\Delta_{\alpha, \beta}$ -spectrum after the selection of fermionic (i, j) parts. The calculated probabilities for each (α, β) -state (i.e., the weight of each part of (α, β)) arranged in order of value of η_{Δ} are shown in Fig.2(c). As we can see, now the probability distribution of potential difference changes and results in nonzero net value of potential difference. The resulting $\Delta_{\alpha, \beta}$ -spectrum is shown in Fig.3(e,f), and the corresponding level spacing ratio follows a distribution between GUE and GSE.

However, it is low efficiency to calculating one-by-one the probability of each part of (α, β) especially for large value of N . Next we introduce a Gaussian-weight-based method. Since there will be $\sim N^2/4$ distinct values of η_{Δ} , which consist the group $\{\eta_{\Delta}\}$. By extracting the mean value and variance of η_{Δ} from the presence $\Delta_{\alpha\beta}$ -spectrum, where we denote as $\mathbf{M} = [\mathbf{QK}^T]^{\eta_{\Delta}}$, and comparing to those quantities of the group $\{\eta_{\Delta}\}$ (where we denote as m_{η} and σ_{η}^2 , respectively), the actual probabilities (weights) for each (α, β) -state can be predicted to high accuracy.

Macroscopically, there will always be more repeating η_{Δ} in the low-value region as can be seen from the η_{Δ} -spectrum, thus the mean value and variance of unbiased η_{Δ} -spectrum will be always lower than the selected one ($\{\eta_{\Delta}\}$). Thus we, in first step, define the mean value m_0 as the maximal value of group η_{Δ} , i.e., $m_0 = N(N-1)$, and making the inner product

$$\mathbf{M} \cdot \mathbf{G}, \quad (3)$$

where $[\mathbf{QK}^T]_{\eta_{\Delta}}$ is the $N(N-1)$ extracted η_{Δ} arranging according to its value. Next,

$$G_{i \in [1, N(N-1) - |\delta_i|]} = \exp\left[\frac{-\left(\{M\}_i - m_{\text{Max}[i] + \lambda_i}\right)^2}{2\sigma_M^2}\right], \quad (4)$$

$$G_{i \in [(N(N-1) - |\delta_i| + 1, N(N-1))]} = 1,$$

where $|\delta_i| = 0$ in the beginning and the mean value $m_{\text{Max}[i] + \lambda_i}$ is the $\text{Max}[i]$ -th element of the ascending-ordered $\{M\}_i$ group. We denote the index as $i = 1, \dots, N(N-1)$ representing the values of η_{Δ} in ascending order. $\sigma_M^2 = \frac{1}{M'} \sum_i^{M'} (M_i - m_0)^2$ is variance of elements in the group $\{M\}_i$ ($i = 1, \dots, M'$) with $M' \leq M$. $\delta_i \in [0, N(N-1))$ is learnable parameter (its variance step is defined according to the feed-back of mean value and variance of the weighted spectrum after the process of last time) which equals to zero in the beginning, and its function here is to restricting the weighted-range to lower- i regions, where has more number of repeating value of η_{Δ} . While other elements of \mathbf{G} are setted as 1. Here the mean value m_i is defined according to the $(N(N-1) - \delta_i)$ -th value of \mathbf{M} , and λ_i is a small quantity which is also a learnable parameter. Its sign $\text{sgn}[\lambda_i]$ is negative when the ratio between mean value (variance) obtained from last iteration (we denote as the l -th learning) and that of the irreducible group $\{\eta_{\Delta}\}$ satisfies $m_l/m_{\eta} \ll \sigma_l^2/\sigma_{\eta}^2$, and its sign should be positive in the opposite case that $m_l/m_{\eta} \gg \sigma_l^2/\sigma_{\eta}^2$. After each time of iteration (learning), the renewed spectrum will be obtained from the matrix \mathbf{M} weighted by the rescaled $\prod_{j=1}^l G_j$ (by softmax process).

The iteration process of learning will stop when the m_l and σ_l^2 are close enough to the standard values m_{η} and σ_{η}^2 , respectively. There are two ways to verify the final results, i.e., the obtained probabilities for each (α, β) -state. First one is comparing the η_{Δ} -spectrum and the level spacing distribution with the exactly calculated one, the second one is to measuring the distance between the predicted probabilities with the exactly calculated ones (denote as p_i^{η}). Instead of using the loss function $L = -\sum_i p_i^{\eta} \ln p_i$, we choose to calculate the mean

value and variance of the group consist of the elements $p_i^{p_i^\eta}$, where both the predict and exact probabilities are arranged in ascending order of η_Δ . While for the exact case, where all the predicted probabilities are the same with the real one, the mean value and variance of the group $\{(p_i^\eta)^{p_i^\eta}\}$ are solely determined by the sample size N , where the mean value ($\sim 2(e^{1/M} - 1)$) exponentially closes to zero and the standard deviation ($\sim 1 - 2(e^{1/M} - 1)$) logarithmically closes to one with the increase of N .

3 Simulations

According to our simulation, the variance of η_Δ spectrum σ_η^2 is lower but close to $\frac{N^4}{16}$ while that of the $\Delta_{\alpha\beta}$ -spectrum is $\sigma_\Delta^2 = \frac{N^2}{4}$ which is quite close to the flavor number of η_Δ -DOF, i.e., $M \sim \frac{N^2}{4}$. Since the η_Δ -DOF is a independent DOF relative to every (i, j) -part, this model is a three-DOF (or three-point all-to-all many-body system) system. As shown in Appendix.B, this can be illustrated in the fermion system by adding another scattering momentum-dependent DOF into the four-point fermion-fermion interacting system, and changes the variance of anti-symmetry tensor from the four-point one ($\sim \frac{1}{4!} = \frac{g_4^2}{4N^3}$) to the three-point one ($\sim \frac{1}{3!} = \frac{g_3^2}{3N^2}$ where $g_n = \sqrt{\frac{n^{n-1}}{(n-1)!}}$ is a constant parameter with dimensions of energy). For example, in Eq.(46) the four Gaussian-independent fermionic indices with $i < j < k < l$ reduce to two (coarse-grained) Gaussian variables (i, k) and j, l (with $i < j$ and $k < l$) which correspond to the fermions before and after scattering, respectively, when it couples to the η_Δ -DOF. The ratio between variance of $\Delta_{\alpha\beta}$ -spectrum and η_Δ spectrum is close to $\frac{\sigma_\Delta^2}{\sigma_\eta^2} \sim \frac{4}{N^2}$. This is because for each fermion part, the probability for M flavors of η_Δ -DOF is $p_\eta = \frac{1}{M} \sim \frac{4}{N^2}$, while the unequivalent distribution of the probabilities (see Fig.3(a)) for each $\Delta_{\alpha\beta}$ (whose mean $\bar{p}_\Delta = \frac{1}{2N(N-1)}$) results in larger uncertainty, and this uncertainty results in stronger thermalization effect (compares to the original one) and smaller variance for the $\Delta_{\alpha\beta}$ -spectrum which is $\leq \frac{N^2}{4}$. In this case the potential difference is a Chi-square variable and has nonzero expectation value. This part of nonzero potential difference corresponds to the UV cutoff in position space as well as the long-wavelength limit for the scattering momenta, which is a signature for the polarons following the Wigner-Dyson distribution. And the resulting distribution is of a intermediate region between the GUE and GSE. While in original $\Delta_{\alpha\beta}$ -spectrum as shown in Fig.1(a,b), the potential difference is a Gaussian variable with zero mean (and thus zero expectation value for the polaronic effect) and the many-body behavior follows the GUE distribution. Also, this case belongs to the four-point-type fermion interaction, with variance $\sigma_{4-p}^2 \sim \frac{4N^2}{4!} = \frac{N^2}{6}$, and its level spacing follows GUE distribution ($\langle r \rangle \sim 0.59$). While the two-point-type fermion interaction (with much stronger thermalization), as shown in Fig.1(c,d), it has a variance which is twice of the four-point one, $\sigma_{2-p}^2 = \frac{N^2}{2!} \frac{2}{3} = \frac{N^2}{3}$, and its level spacing follows GSE distribution ($\langle r \rangle \sim 0.67$). Then it is reasonable for the intermediate case we studied here, whose variance $\sigma_\Delta^2 \sim \frac{N^2}{4}$ is between the two-point one and four-point one, and follows the ensemble between GUE and GSE with $\langle r \rangle = 0.63 \sim 0.65$. More critically, the variance σ_Δ^2 is in fact N -dependent even for $N \rightarrow \infty$. If we treating it as an inner product by four-point variance and two-point variance weighted by different probabilities, an experimental expression could be

$$\sigma_\Delta^2 = (1 - \frac{1}{\ln N^2} [\sigma_{2-p}^2, \sigma_{4-p}^2] \cdot \text{Softmax}[1, 2]) \approx (1 - \frac{1}{\ln N^2} (0.2689\sigma_{2-p}^2 + 0.731\sigma_{4-p}^2)). \quad (5)$$

For example, for $N = 100, 150, 200$, the corresponding variances $\{\sigma_{2-p}^2, \sigma_\Delta^2, \sigma_{4-p}^2\}$ are $\{3333.3, 1954, 1666.5\}$, $\{7500, 4355, 3750\}$, and $\{13421, 7674.1, 6666, 6\}$, respectively. There is a tendency which is persistent for arbitrarily large- N : the variance of such intermediate state depends on both the other

two variances, σ_{2-p}^2 and σ_{4-p}^2 whose values can be solely determined in large- N limit, and with N increasing, the σ_{Δ}^2 will more and more close to the four-point one σ_{4-p}^2 (compared to σ_{2-p}^2) with a decreasing but never vanished velocity. This indeed reflects a spontaneous localization, and the suppressed thermalization with the increasing N .

4 Mathematical principle behind the learning-algorithm designing

4.1 Algorithm

During the steps of automatic iterations, the criterion is to matching the mean value and variance of the predicted spectrum with the reduced one (irreducible group, which has much small sample size). We using the rule that for every weighted group that containing only two elements, its variance will never be changed when we modify there corresponding weights, even if the summation of there corresponding weights not equals to one, by the mean value will changes in this process.

For example, for a group k_1, k_2 weighted by w_1, w_2 , the variance reads

$$\sigma^2 = \frac{\sum_i w_i (k_i - m_k)^2}{\sum_i w_i - \frac{\sum_i w_i^2}{\sum_i w_i}}, \quad (6)$$

where $m_k = \sum_i k_i w_i / \sum_i w_i$ is the weighted mean value. This expression is equivalent to replacing w_2 by $(1 - w_1)$ and omit the $\sum_i w_i$ in the denominator, i.e., $\sigma^2 = \frac{\sum_i w_i (k_i - m_k)^2}{1 - \sum_i w_i^2}$. Thus next we consider only the case $\sum_i w_i = 1$. Then we introduce another one with modified weight distribution $\{w'_1, w'_2\} := \{w_1 + w_d, w_2 - w_d\}$. These two groups have the same variance

$$\sigma^2 = \frac{1}{2}(k_1 - k_2)^2 = \frac{(k_1 - k_2)^2 \prod_i w_i}{1 - \sum_i w_i^2} = \frac{(k_1 - k_2)^2 (\prod_i w_i - w_d^2 + w_d(1 - 2w_1))}{1 - \sum_i w_i'^2}. \quad (7)$$

This can be explained using the method we discussed in Ref.[1], i.e., expressing this common variance σ^2 in terms of a limiting result of the infinitely scaled variable χ (the detailed form of this variable does not have to know), which has the form $\sigma^2 := \lim_{\chi \rightarrow \infty} f = \frac{f}{1 - \partial_{\chi} f}$. In above expression the summation of squared weights of these two groups can be treated as there corresponding derivative terms with respect to χ ,

$$\sum_i w_i^2 = 1 - 2w_1(1 - w_1), \quad \sum_i w_i'^2 = 2(-w_d^2 + (1 - w_1)w_1 + w_d(1 - 2w_1)). \quad (8)$$

For first group, by defining $\prod_i w_i = w_1(1 - w_1) := f_{\chi}$, we have

$$\begin{aligned} \frac{1}{2} &= \lim_{\chi \rightarrow \infty} f_{\chi} = \frac{f_{\chi}}{1 - \partial_{\chi} f_{\chi}}, \\ 1 - 2f_{\chi} &= \partial_{\chi} f_{\chi}, \\ \frac{1}{2}(k_1 - k_2)^2 &= \lim_{\chi \rightarrow \infty} (k_1 - k_2)^2 f_{\chi}, \\ 1 - 2f_{\chi} &= \partial_{\chi} [(k_1 - k_2)^2 f_{\chi}]. \end{aligned} \quad (9)$$

There are two possible cases which correspond to different representations. The first one is the representation in unit of $(k_1 - k_2)^2$ which is independent with χ . This case will leads to $w_i = \frac{1}{2} \pm \frac{i}{2}$. The second one is the representation in unit of $\lim_{\chi \rightarrow \infty} f_{\chi} = \frac{1}{2}$. In this representation, the acceptable results, $w_i = \frac{1}{2}$ can be solved. Note that for this case, the derivative term $\partial_{\chi} f_{\chi}$ in the second line of above expression indeed corresponds to $\partial_{\chi} w_1 =$

$(1 - w_1)$ and $\partial_\chi w_2 = \partial_\chi(1 - w_1) = w_1$, which mean the variable χ is scalable by 1 (which is no more a constant here), and $\partial_\chi 1 = 1$. Here $1 = e^{i(2\pi - 0^+)}$, where 0^+ denotes an infinitely small shiftment in phase and generate the imaginary part into the previous representation, and the cutoff of this infinitely small imaginary part (which is the UV cutoff in momentum space if we projecting this imaginary part into the position space) determines directly the largest quantity that could be independent with χ , i.e., the unit quantity in this representation ($1/2$). Thus more rigorously we have $\partial_\chi f_\chi = 1^2 - 2f_\chi$ with $1^2 \neq 1$ and $\partial_\chi 1 \neq \partial_\chi 1^2$. Here this cutoff is necessary to fix the tolerance of whole system, i.e., $\partial_\chi \frac{1}{2} = \left| \frac{1}{2} - \frac{1}{2 + \frac{1-1^2}{f_\chi}} \right| = 0$. Substituting the second line of above expressions into the expanded expression in the last line, we have

$$\partial_\chi(k_1 - k_2)^2 = \frac{1 - 2f_\chi}{f_\chi}[1 - (k_1 - k_2)^2] = \frac{\partial_\chi f_\chi}{f_\chi}[1 - (k_1 - k_2)^2]. \quad (10)$$

In the mean time, due to the invariant property of the infinite scale, $\partial_\chi \lim_{\chi \rightarrow \infty} f_\chi = 0$, the first line of Eq.(9) results in the relation

$$\frac{1 - 2f_\chi}{2f_\chi} = -f_\chi \partial_\chi \frac{1}{2f_\chi}. \quad (11)$$

Substituting this into Eq.(10), we can obtain

$$\frac{1 - (k_1 - k_2)^2}{\partial_\chi(k_1 - k_2)^2} = \frac{1}{2} \frac{-1}{f_\chi \partial_\chi \frac{1}{2f_\chi}} = \frac{f_\chi}{\partial_\chi f_\chi}. \quad (12)$$

Thus we can make sure that there must be another $\prod_i w_i$ -related variable χ' satisfying

$$\begin{aligned} \lim_{\chi' \rightarrow \infty} f_{\chi'} &= \frac{\partial f_\chi}{\partial(k_1 - k_2)^2}, \\ \partial_{\chi'} f_{\chi'} &= (k_1 - k_2)^2. \end{aligned} \quad (13)$$

Using the property $\frac{f_\chi}{\partial_\chi f_\chi} \equiv \lim_{\chi \rightarrow \infty} f_\chi \frac{f_\chi}{\lim_{\chi \rightarrow \infty} f_\chi - f_\chi}$, we have

$$\begin{aligned} f_\chi &= \frac{-\partial_\chi f_\chi}{1 - \partial_\chi f_\chi} \frac{1}{\partial_\chi \frac{1}{2f_\chi}}, \\ &= \frac{\partial f_\chi}{\partial(k_1 - k_2)^2} [1 - (k_1 - k_2)^2]. \end{aligned} \quad (14)$$

Combined with Eq.(10), we obtain the following form of the limiting scale

$$\lim_{\chi \rightarrow \infty} f_\chi = \frac{1}{2} = f_\chi - f_\chi^2 \partial_\chi \frac{1}{2f_\chi}. \quad (15)$$

Besides, using Eq.(12) and the derivative of the ratio between two limits $\frac{\lim_{\chi \rightarrow \infty} [(k_1 - k_2)^2 f_\chi]}{\lim_{\chi \rightarrow \infty} f_\chi} = (k_1 - k_2)^2$, we obtain

$$\begin{aligned} \partial_\chi \ln \frac{1}{\lim_{\chi \rightarrow \infty} f_\chi} &= \partial_\chi \ln 2 \\ &= \frac{\partial_\chi f_\chi}{f_\chi} \frac{1 - (k_1 - k_2)^2}{(k_1 - k_2)^2} \\ &= \frac{\partial_\chi(k_1 - k_2)^2}{(k_1 - k_2)^2}. \end{aligned} \quad (16)$$

Thus we have, $\frac{\partial_\chi 2}{2} = \frac{\partial_\chi (k_1 - k_2)^2}{(k_1 - k_2)^2}$, thus in the limit of $\partial_\chi 2 \rightarrow 2$, $(k_1 - k_2)^2 \rightarrow e^{i(2\pi - 0^+)} = e^\chi$ and $\frac{\partial_\chi (k_1 - k_2)^2}{(k_1 - k_2)^2 - 1} \rightarrow \frac{\partial_\chi (k_1 - k_2)^2}{(k_1 - k_2)^2}$. To looking for real solution, in this limit we have $(k_1 - k_2)^2 = e^\chi \sim 1$, i.e., $\lim_{\chi \rightarrow \infty} |k_1 - k_2| \gg |k_1 - k_2|$. This fact reveals the reason why the variance of such binary group will always keep invariant when we modify the weight distribution or change the value of elements, as long as the distance between two elements is invariant. This is consistent with the fact that $|k_1 - k_2| \propto \delta\chi$ as they all describe the distance in the position space, while the corresponding long wavelength limit in momentum space after fourier transformation can be realized by the factor $[1 - (k_1 - k_2)^2]^{-1}$. Also, the unit quantity expressed in terms of the limiting relation as shown in eq.(15) allows the easier derivation along the distances in the position space. For example, if we consider beyond the binary groups by replacing $f_\chi = w_1(1 - w_i)$ as the variance for the binary group in its position, then the $[\partial_\chi \frac{1}{2f_\chi}]^{-1}$ -term in Eq.(15) can indeed be regarded as the variance of another group (with more elements) in position next to the former one. To illustrating this, we set the binary group in the first position as (k_1, k_N) whose variance denoted as v_1 , and the one in the next position as $(k_1, k_1 + 1, k_N - 1, k_N)$ whose variance denoted as v_2 . The other groups with more elements are arranged in the same manner. Then the slope in the position space is equivalent to the variance ratio $\frac{v_1 - v_2}{v_2 - \frac{v_2^2}{v_1}} = \frac{v_1}{v_2}$, where $(v_2 - \frac{v_2^2}{v_1})$ is the smallest step length here appearing in the same form with Eq.(15), i.e., the IR cutoff in the position space. Such unit length as well as the slope are not invariant between arbitrarily two positions with different numbers of element, and this length reduces to zero efficiently for higher-order position derivative. For example, by setting $k_N = 13$, the first to fourth-order derivative are -6.4918 , 0.84579 , 0.040513 , 0.0093128 , respectively, and the highest-order one (the twelfth-order derivative) is 0.000030169 .

It can be checked that, in this representation, where both the elements and weights are dependent with χ , the real solution of weights $w_i = \frac{1}{2} = \partial_\chi f_\chi = (k_1 - k_2)^2 [1 - \frac{1}{2 \lim_{\chi \rightarrow \infty} (k_1 - k_2)^2}] (f_\chi = \frac{1}{4})$ can be obtained, where $\partial_\chi \frac{1}{2f_\chi} = -4$. In the mean time the infinite χ corresponds to the simultaneous scalings of $w_i \rightarrow \frac{1}{2}$ and $w_d^2 \rightarrow 0$ for the second group, which results in the same result of variance. Thus for such kind of binary groups, we can solely modify the mean value and keep the variance be invariant. To modify the variance, the simplest way is by introducing the third element, which can be viewed as a collection of all the other elements in the reducible group $\{\alpha, \beta\}$ other than the two elements in both sides of the position that the algorithm kernel working on. Once a position is initially determined, the elements in two sides of this position will be treated as a part of binary (summation of weights is one), then the mean value can be increased by giving more weight to the right-side one, which corresponds to larger value of η_Δ . Then other elements enter this group play the role of third element to available the adjustment for the variance. In Eq.(4), the learnable mean value $m_{i+\lambda_i}$ at position $i = i'$ can be adjusted with the range of $[\{M\}_{i'}, \{M\}_{N(N-1)}]$. As the subscript of this learnable mean parameter decreasing from the largest one $N(N-1)$ (corresponds to the position at the end of spectrum), the resulting mean value and variance of the updated η_Δ -spectrum will both be increased at first and then keep decreasing until the subscript decreases to $i = i'$. During this process, there will be a certain position will the mean value is enhanced while the variance is reduced (compares to the former spectrum before the update of parameters).

In this way, the learnable-parameter-dependent step lengths control the positions where the algorithm modifies the weight distribution step-by-step, and the ratio between mean value and variance can be modified until the spectrum exhibits features match enough to the one corresponding to the irreducible group.

4.2 Criterion

Except the above-introduced method to estimate the degree of coincidence between the predicted mean value and variance with the exact ones, there is another criterion using the β_{en} -factor ($\beta_{en} = 1, 2, 4$ for GOE, GUE, and GSE ensembles). As the joint probability density function for Gaussian ensembles[39] satisfies

$$P_{joint} = C_{\beta,N} \prod_{i<j} |k_i - k_j|^{\beta_{en}} e^{-\frac{1}{2} \sum_i^N (k_i - m_k)}, \quad (17)$$

where the normalization parameter reads

$$C_{\beta,N} = \frac{1}{(2\pi)^{N/2}} \prod_j^N \frac{\Gamma[1 + \frac{\beta_{en}}{2}]}{\Gamma[1 + j \frac{\beta_{en}}{2}]}. \quad (18)$$

We note in advance that, as can be seen from Eq.(6) in the above subsection, we are using the bias-corrected sample variance throughout this paper. Then according to the above-introduced algorithm, we start with an ascending-ordered original η_Δ -group (unreducible) $\{M\}_{i=1, \dots, N(N-1)} := \{k_1, \dots, k_{N(N-1)}\}$ following GUE distribution (whose mean value and variance are denoted as m_o and σ_o^2 , respectively), in first round of learning, we obtain the weight distribution for all elements by lifting the mean value to the largest one (k_{max}), then this results in a new variance

$$\begin{aligned} \sigma_M^2 &= \frac{\sum_i^{N(N-1)} (k_i - k_{max})^2}{N(N-1)[1 - \frac{1}{N(N-1)}]} = \frac{\sum_i^{N(N-1)} (|k_{max} - m_o| + |k_i - m_o| \theta(k_o - k_i) - |k_i - m_o| \theta(k_i - k_o))^2}{N(N-1)[1 - \frac{1}{N(N-1)}]} \\ &= \frac{\sigma_o^2(N(N-1) - 1) + N(N-1)|m_o - k_{max}|^2}{N(N-1) - 1}, \end{aligned} \quad (19)$$

where the factor $|m_o - k_{max}|^2$ can be much easily obtained from the summation of all elements as well as the two mean values

$$|m_o - k_{max}|^2 = N(N-1)[(k_{max}^2 - m_o^2) + 2(m_o - k_{max}) \sum_i k_i], \quad (20)$$

Also, the summation of squared elements can be obtained $\sum_i k_i^2 = \sigma_o^2(N(N-1) - 1) - N(N-1)m_o^2 + 2m_o \sum_i k_i$, and then we can know that all the antisymmetry-allowed combinations ($i < j$) in the second term of above joint probability density function have an available summation

$$\sum_{i<j} |k_i - k_j|^2 = \sum_i k_i^2 (N(N-1) - 1) - [(\sum_i k_i)^2 - \sum_i k_i^2]. \quad (21)$$

Then in this algorithm, we letting each element (eigenvalues) in the group $\{M\}_i$ weighted by the factors $\text{softmax}\{e^{-(k_i - k_{max})^2 / (2\sigma_M^2)}\}_i$ (using the variance σ_M^2 defined-above), then if we substituting the resulting variance of these weighed eigenvalues back to the joint eigenvalue probability density function of the original one in GOE ensemble (with the normalization constant $C_{2,N}$), we can obtain an increased factor of β_{en} (between 2 and 4) for the Lebesgue measure[38], i.e., the second term of P_{joint} . Next we rewrite the maximal index in the group $\{M\}_i$ as $N(N-1) \equiv n$ for simplicity in notation.

We know the antisymmetry product $\prod_{i<j} |k_i - k_j|^{\beta_{en}}$ equivalents to the van der Monde determinant,

$$\prod_{i<j} |k_i - k_j|^{\beta_{en}} = (\text{Det} \begin{pmatrix} 1 & k_1 & k_1 & \cdots & k_1 \\ 1 & k_2 & k_2^2 & \cdots & k_1^{n-1} \\ \dots & \dots & \dots & \dots & \dots \\ 1 & k_n & k_n^2 & \cdots & k_N^{n-1} \end{pmatrix})^{\beta_{en}}. \quad (22)$$

To clarify the effect of the variant β_{en} on this term, we using the tridiagonal matrix lemmas[39]. Assuming the above van der Monde matrix can be transformed into a tridiagonal symmetry matrix with diagonal element T_d and subdiagonal elements $T_i (i = 1, \dots, N - 1)$ arranged in the form

$$T_n = \begin{pmatrix} t_d & t_{n-1} & 0 & \cdots & 0 & 0 \\ t_{n-1} & T_d & t_{n-2} & \cdots & 0 & 0 \\ 0 & t_{n-2} & T_d & \cdots & 0 & 0 \\ \cdots & & & & & \\ 0 & 0 & 0 & \cdots & t_1 & t_d \end{pmatrix}. \quad (23)$$

For this matrix, we have $\text{Det}T_n = t_d \text{Det}T_{n-1} - t_{n-1}^2 \text{Det}T_{n-2}$, where t_{n-1} is the $(n-1) \times (n-1)$ lower right-corner submatrix of T_N and $k_j^{(n-1)}$ are its eigenvalues. There is another relation[39] $\prod_i (k_j^{(m)} - k_i^{(n)}) = (k_j^{(m)} - t_d) \prod_i (k_j^{(m)} - k_i^{(n-1)}) - t_{n-1}^2 \prod_i (k_j^{(m)} - k_i^{(n-2)})$, where $m \in [2, n]$ with corresponding $j \in [1, m]$. For $m = n$, both sides of this equation are zero.

For ascending ordered eigenvalues of $T_M (M = n, n-1, \dots, 2)$, the total number of eigenvalues for these (sub)matrices satisfy $\sum_{i=1}^{M+1} k_i^{(M+1)} - \sum_{j=1}^M k_j^{(M)} = t_d$, i.e., the summation of all eigenvalues for two adjacent (sub)matrices always differed by the diagonal element t_d . Also, $\prod_{i=1}^{(n)} (k_i^n - k_1^{(M')}) = \prod_{i=1}^n (k_i^{(n)} - k_{M'}^{(M')})$ where $M' = N-1, \dots, 2$, and $k_1 (k_{M'})$ corresponds to the smallest (largest) eigenvalue of the submatrix $T_{M'}$. We also know that $\prod_{i,j} (k_i^{(N)} - k_j^{(N-1)}) = \prod_i^{n-1} t_i^{2i}$, and $\prod_{i,j} (k_i^{(n)} - k_j^{(n-2)}) = t_1^2 \prod_i^{n-1} t_i^{2i}$.

The product of the eigenvalue permutations of T_N in ensemble β_{en} satisfies the following relation according to the algebraic fact

$$\prod_{i < j} |k_i - k_j|^{2\beta_{en}} = \frac{\prod_{i=1}^{n-1} t_i^{2i}}{\prod_{i=1}^n Q_i^{2\beta_{en}}} = \frac{\prod_{1 \leq i < j \leq n-1} (k_i^{(n)} - k_j^{(n-1)})}{\prod_i Q_i^{2\beta_{en}}}, \quad (24)$$

where $\prod_i Q_i$ is the product of elements in the first row of eigenvector matrix of T_n .

According to the above discussion and simulations, we know that the self-modified parameters lifting the variance of eigenvalues by changing the weight distribution and thus lifting the ensemble index in normalized Lebesgue measure (i.e., the product of the eigenvalue permutations) of the joint eigenvalue probability density function. The ensemble index β_{en} will finally be increased from 2 to a larger one β'_{en} which is between 2 and 4 and reveals a distribution between GUE and GSE. During this process, the changes of product term $\prod_{i < j} |k_i - k_j|^{2\beta_{en}}$ can be visualized by the product of the eigenvectors $\prod_{i=1}^n Q_i^{2\beta_{en}}$. When the change $\beta_{en} \rightarrow \beta'_{en}$ happen, the variance of $\prod_{i=1}^n Q_i^{2\beta_{en}}$ reads

$$\prod_i Q_i^{2\beta} \left(\prod_i Q_i^{2(\beta'_{en} - \beta_{en})} - 1 \right) = \frac{\prod_i t_i^{2i\beta_{en}} \left(\prod_i t_i^{2i(\beta'_{en} - \beta_{en})} - \prod_{i < j} |k_i - k_j|^{2(\beta'_{en} - \beta_{en})} \right)}{\prod_{i < j} |k_i - k_j|^{2\beta'_{en}}}. \quad (25)$$

Then if we rescale the change $\beta_{en} \rightarrow \beta'_{en}$ to another one: $\beta'_{en} \rightarrow \infty$, which can be realized by another two scalings that happen simultaneously: $\beta_{en} \rightarrow \infty - |\beta_{en} - \beta'_{en}|$ and $\prod_i Q_i^2 \rightarrow 0$ (and thus β_{en} and β'_{en} are still independent with each other). From above equation, we can define the following function of β'_{en}

$$f_{\beta'_{en}} := \frac{\prod_{i < j} |k_i^{(n)} - k_j^{(n)}|^{2(\beta'_{en} - \beta_{en})} - \prod_i t_i^{2i\beta_{en}} \left(\prod_i t_i^{2i(\beta'_{en} - \beta_{en})} \right)}{\prod_{i < j} (k_i^{(n)} - k_j^{(n)})^{2\beta'_{en}}}. \quad (26)$$

Then we have

$$\frac{f_{\beta'_{en}}}{\lim_{\beta'_{en} \rightarrow \infty} f_{\beta'_{en}}} = 1 - \partial_{\beta'_{en}} f_{\beta'_{en}}, \quad (27)$$

where

$$\begin{aligned}\lim_{\beta'_{en} \rightarrow \infty} f_{\beta'_{en}} &= \prod_{i < j} (k_i^{(n)} - k_j^{(n)})^{-2\beta_{en}}, \\ \partial_{\beta'_{en}} f_{\beta'_{en}} &= \prod_i Q_i^{2\beta'_{en}} \frac{\ln \prod_i Q_i^2}{\prod_i t_i^{2i\beta}}.\end{aligned}\tag{28}$$

Since the above rescaling actions endow the β_{en} -dependence (instead of β'_{en}) to the term $\prod_i Q_i^{2\beta'_{en}}$, i.e., $-\ln \prod_i Q_i^{2\beta'_{en}} \equiv \prod_{i < j} (k_i^{(n)} - k_j^{(n)})^{2\beta_{en}}$, which scales to infinity accompanied by $\beta'_{en} \rightarrow \infty$, and this equality will not be broken even before the limit $\beta'_{en} \rightarrow \infty$ is arrived, i.e., it is valid even when the β'_{en} -dependence of $f_{\beta'_{en}}$ not yet fade away.

4.3 Further explanation in scaling

Like in conformal field theories[], the decrease of effective number of DOF under renormalization group is important to gain further understanding for the complex systems. Here we add more detailed explanations about the scaling behaviors in above subsection. Firstly we replacing the normal ensemble change $\beta_{en} = 2 \rightarrow \beta'_{en} \in (2, 4)$ by another ones: $\beta'_{en} \rightarrow \infty$; $\prod_i Q_i^2 \rightarrow 0$, $\prod_{i < j} (k_i^{(n)} - k_j^{(n)})^{2\beta_{en}} \rightarrow \infty$. Under this, the independence between $\beta_{en}(Q_i)$ with β'_{en} are preserved just like the original case. But in the mean time, we have to endow the Q_i -related product term with the β_{en} -dependence, in other world, this combine the Q_i and β_{en} DOFs. To make sure all these requirements are metted, as the β'_{en} scales to infinity, β_{en} has to scale to $(\infty - (\beta'_{en} - \beta_{en}))$. There is an essential logical relation between β_{en} and β'_{en} . As β'_{en} scales to infinity at first, $\beta'_{en} + \infty \rightarrow \infty$, the locked β_{en} scales as $\beta_{en} \rightarrow \beta_{en} + \infty - (\beta'_{en} - \beta_{en})$. That means in any moment, the detail value of β_{en} cannot be obtained before $(\beta'_{en} - \beta_{en})$, i.e., the derivative of β_{en} with β'_{en} , is known. Thus we have

$$\frac{\partial \beta_{en}}{\partial \beta'_{en}} = \frac{\infty - (\beta'_{en} - \beta_{en})}{\infty},\tag{29}$$

where the numerator is the variance of β_{en} which can found to be depends on itself only. We have

$$\beta_{en} = \infty - (\beta'_{en} - \beta_{en}) = \frac{\infty - (\beta'_{en} - \beta_{en})}{\frac{\infty}{\beta'_{en} - \beta_{en}}} \frac{\partial(\beta'_{en} - \beta_{en})}{\partial(1 - \mathbb{1})},\tag{30}$$

where $\mathbb{1} = (\beta'_{en} - \beta_{en}) - \frac{(\beta'_{en} - \beta_{en})^2}{\beta'_{en}}$ is the unit step in this derivative and this derivative can be obtain using the method we introduced in Sec.4.2,

$$\frac{\partial(\beta'_{en} - \beta_{en})}{\partial(1 - \mathbb{1})} = \frac{\infty - (\beta'_{en} - \beta_{en})}{\mathbb{1}} = \frac{\infty}{\beta'_{en} - \beta_{en}}.\tag{31}$$

Thus that means the $\mathbb{1}$ and 1 in the denominator of first line are in fact not in the same domain, and once they appear together through the algebra-allowed limiting-scale-assisted domain transition, we can in fact write $\mathbb{1}$ more strictly as $1^- := e^{i(2\pi - 0^-)}$, and similar to the derivative of $\frac{\partial \beta_{en}}{\partial \beta'_{en}}$, their relations can be understood by $1 \mapsto \beta'_{en} + \infty$, $\mathbb{1} \mapsto \infty$. We can resubstituting this β_{en} back to the above expression of $\frac{\partial \beta_{en}}{\partial \beta'_{en}}$ repeatly,

$$\frac{\partial(\beta'_{en} - \beta_{en})}{\partial(1 - \mathbb{1})} = \frac{\partial - \frac{\partial(\beta'_{en} - \beta_{en})}{\partial(1 - \mathbb{1})}}{\partial(1 - \mathbb{1})} = \dots,\tag{32}$$

and finally we can obtain the vanishing variance of β_{en} at a certain order N : $\frac{\partial^{(N)}(\beta'_{en} - \beta_{en})}{\partial(1 - \mathbb{1})^N} = 0$, and whatever which IR cutoff we set (through this N), the variance of β_{en} will vanishes faster than the one in its next hierarchy β'_{en} .

Similarly, the derivative of the function $f_{\beta'_{en}}$ can be rewritten as

$$\frac{\partial f_{\beta'_{en}}}{\partial \beta'_{en}} = \frac{\prod_i Q_i^{2\beta'_{en}}}{\partial(1 - \mathbf{1}')} \quad (33)$$

where

$$\mathbf{1}' = \prod_i Q_i^{2\beta'_{en}} - \frac{\prod_i Q_i^{4\beta'_{en}}}{\prod_i Q_i^{2\beta'_{en}}}, \quad (34)$$

and we also have

$$\prod_i Q_i^{2\beta'_{en}} = 2(\mathbf{1}' + \prod_i Q_i^{2\beta'_{en}}) - 1. \quad (35)$$

4.4 Provenance of an essential formula

Just like the Eq.(15) and the unit quantities appear in above subsection, the variance (or global-invariance in its own hierarchy of the step length (IR cutoff in position space) in each position is essential for the all of the above discussions as well as the algorithm designing in this paper. A hierarchy-dependent step length allows much easier and faster derivation (estimation of local gradient) which largely increases the efficiency during the optimizations for every positions (i.e., the weight for every eigenvalues in the target matrix). As shown in sec.4.1, this can be denoted as

$$\frac{\partial b}{\partial a} = \frac{a - b}{\mathbf{1}} = \frac{a}{b}, \quad (36)$$

where b and a are the target position and the next position, respectively, and the unit length reads $\mathbf{1} = b - \frac{b^2}{a}$. It can be seen that, the target eigenvalue b here indeed corresponds to the function f_χ in Eq.(15) or $(\beta'_{en} - \beta_{en})$ in the unit length in Eq.(30), while a equivalents to $(\partial_\chi \frac{1}{2f_\chi})^{-1}$ in Eq.(15). Note that for Eq.(30), the eigenvalue of the next position a corresponds to the $(1 - \mathbf{1})$, which equals to ∞ with respect to β_{en} , since β_{en} is latter in "time" for the scaling, as we explained in above.

For Eq.(36) we used here, we assume b is a derivative result of the real variable x (thus the limit of b under scaling $x \rightarrow \infty$ is also a real constant), then we have $a = [\partial_x \frac{\lim_{x \rightarrow \infty} b}{b}]^{-1} = \frac{b^2}{b - \lim_{x \rightarrow \infty} b} = b \frac{\partial_x b - 1}{\partial_x b}$. Note that since x is real, every real constants are not dependent with x . This will not be the case when we using b as a variable during the derivative.

Then we have

$$\frac{\partial b}{\partial a} = \frac{a}{b} + b \partial_b \frac{a}{b} = \frac{\partial_x b - 1}{\partial_x b} + b \partial_b \frac{\partial_x b - 1}{\partial_x b} = \frac{\partial_x b}{\partial_x b - 1}. \quad (37)$$

There are several relations that can be proven rigorously. For step length defined in terms of the complex variable b , $\mathbf{1} \equiv \frac{\partial_x b}{\partial_x b}$, we have

$$\begin{aligned} \partial_b \mathbf{1} &= \frac{1}{a} = \frac{\partial_x b}{b(\partial_x b - 1)}, \\ \partial_b \frac{1}{\partial_x b} &= \frac{a}{b^2} = \frac{\partial_x b - 1}{b \partial_x b}, \end{aligned} \quad (38)$$

$$\partial_b(\partial_x b) = \partial_b \mathbf{1} (\partial_x b - (\partial_x b - 1)^2) = \frac{(\partial_x b)^2}{b(\partial_x b - 1)} - \frac{\partial_x b - 1}{b} \partial_x b,$$

where the last line can be proved by the second line that $\partial_b \frac{1}{\partial_x b} = \frac{\partial_b \mathbf{1}}{\partial_x b} - \frac{\partial_b(\partial_x b)}{(\partial_x b)^2}$. Rewriting the first line as $\partial_b \mathbf{1} = 1' - \frac{1}{\lim_{b \rightarrow \infty} \mathbf{1}}$, where $1' = \frac{1}{\lim_{b \rightarrow \infty} \mathbf{1}} + \partial_b \mathbf{1} \neq 1$. Then according to the independence with b for the term $\lim_{b \rightarrow \infty} \mathbf{1}$, we have

$$1' - \frac{\partial 1'}{\partial \mathbf{1}} = \partial_b \mathbf{1} - \frac{\partial_b^{(2)} \mathbf{1}}{\partial_b \mathbf{1}}. \quad (39)$$

By the above equations, it can be deduced that $\partial_b(2)1 = 0$. thus we further obtain $\partial_b(\lim_{b \rightarrow \infty} 1) = \partial_b^{(2)}1(\frac{\partial 1'}{\partial 1})^2 = 0$, and $1' = \partial_b 1 + \frac{1}{\lim_{b \rightarrow \infty} 1}$. Thus $1'$ defined here is completely related to the dependence of 1 with b as well as to what extent this dependence will be still persist. In other word, $1'$ is a measurement of stubbornness of such dependence (correlation) for the hierarchy next by it.

4.5

To see inter-relations between different hierarchies, we intruduce another limit $\lim_{x \rightarrow \infty^-} f_x$ for function f_x . As the step length (limiting result) can be invariant only in its own frame, we have $\partial_x 1 = 0$ and $\partial_x \mathbb{1} \neq 0$ in the frame consists of the steps 1 , where $\mathbb{1}$ and 1 are of different hierarchies, and $\mathbb{1} > 1$ since as x scales over the infinity (we have approximately the variance $\delta x \sim 1/x$), the x -independence of the step length in first hierarchy (with step length 1) disappear and it requires a larger step length ($\mathbb{1}$) to keep this invariance. That is why we have $\partial_x 1 = 0$ and $\partial_x \mathbb{1} \neq 0$ in the first hierarchy.

Then in this hierarchy we have two expressions,

$$\begin{aligned} \lim_{x \rightarrow \infty} f_x &= \frac{f_x}{1 - \partial_x f}, \\ \lim_{x \rightarrow \infty^-} f_x &= \frac{f_x}{\mathbb{1} - \partial_x f} = \frac{\mathbb{1}}{f_x}. \end{aligned} \quad (40)$$

By cutting at the second order $\partial_x^{(2)} f_x = 0$ for the first hierarchy, we can consistently obtain the following results

$$\begin{aligned} \partial_x \frac{\mathbb{1}}{f_x} &= \partial_x f_x \left(\frac{1}{\mathbb{1}} - \frac{\mathbb{1}}{f_x^2} \right) = \partial_x^{(2)} f_x \frac{\mathbb{1}^2}{f_x^3}, \\ \partial_x f_x &= \mathbb{1} - \frac{\mathbb{1}^2}{f_x^2}. \end{aligned} \quad (41)$$

Specifically, the "shifted" limiting term $\lim_{x \rightarrow \infty^-} f_x$ satisfies the following relations, basing on the step length in this frame $\lim_{x \rightarrow \infty} f_x = f - f^2/\mathbb{1}$,

$$\lim_{x \rightarrow \infty^-} f_x = \frac{\mathbb{1}}{f_x} = \frac{\partial_x f_x - 1}{\partial_x f_x} = \frac{\partial f_x}{\partial \mathbb{1}}. \quad (42)$$

It can be seem that, the cutoff is not at the second order anymore for the next hierarchy consists of the steps $\mathbb{1}$, but here the results are always consistent with the first hierarchy, e.g., the values (and x -independence) of $\lim_{x \rightarrow \infty} f_x$ and $\partial_x 1$ are never being changed. Also, from the two expressions in Eq.(40), we can obtain the same value of the derivative $\partial_x f_x$. This is because the deviation induced by the shifted cutoff for the frame in terms of $\mathbb{1}$ will always be canceled by the x -dependence of $1'$ (and $\lim_{x \rightarrow \infty} f_x$) in its own frame. All these are guaranteed by the following strict relations

$$\begin{aligned} f_x^2 - \mathbb{1}^2 &= \frac{\mathbb{1} f_x}{\mathbb{1} - f_x}, \\ (f_x - \mathbb{1})^2 &= \frac{-\mathbb{1} f_x}{\mathbb{1} + f_x} = \left(\frac{\mathbb{1} f_x}{\mathbb{1}^2 - f_x^2} \right)^2 \end{aligned} \quad (43)$$

which can be rigorously verified that consistent with the above expressions. This reveals the

more clear relation between f_x and $\mathbb{1}$,

$$\begin{aligned} f_x &= \mathbb{1} + \frac{f}{\partial_x f_x}, \\ \mathbb{1} &= f_x - \frac{f}{\partial_x f_x}, \\ \partial_x \mathbb{1} &= \partial_x f_x + \frac{f_x}{\mathbb{1}} = \mathbb{1} - \frac{f_x^2}{\mathbb{1}} + \frac{f_x}{\mathbb{1}}, \end{aligned} \tag{44}$$

which can be verified by substituting Eqs.(??). Since in the frame of next hierarchy, it still has $\partial_x \mathbb{1} = 0$, the derivative of Eq.(42) reads

$$\partial_x \left(\lim_{x \rightarrow \infty^-} f_x \right) = \partial_x \left(1 - \frac{1}{\partial_x f_x} \right) = -\frac{1}{(f_x - \mathbb{1})^2}, \tag{45}$$

which can be verified by the Eq.(43).

5 Conclusion

We reveal the relation between UV cutoff of polaronic momentum Λ_q and its SYK behavior. The SYK behavior of a polaron system, as well as the relation between scattering momentum and the related statistical behaviors has rarely been investigated before. By projecting to a 2d square lattice, The algorithm designed by us allow the automatically optimization and prediction for the resulting spectrum. In this 2d lattice model with position space representation, the emergent nonzero expectation value of site potential difference $\Delta_{\alpha\beta}$ shows the existence of polaron. For eigenvalues arranged in ascending order in the position space, the learning program devotes to predict the weight distribution of each eigenvalue in the final spectrum, which is realized by modifying the relative distance between each pair of the two elements (groups) in both sides of the selected positions. Indeed this is equivalent to modifying the step length for each position, i.e., the IR cutoff in the position space, but this cutoff is no longer a invariant constant here. One of the obvious advance of this is the much easier estimation of the derivative of potential difference in each position, which is directly related to the variance as well as mean value of the final spectrum. Also, the large distance in the lattice position space (like the scaled variable χ) corresponds to the long wavelength limit in the momentum space.

In momentum space, as the polaron emerges at the pole of scattering amplitude, the polaronic momentum q , which is also the relative momentum during scattering between impurity and majority particles (or holes), reads $q = ia^{-1}$. The quantity qa is also an important characteristic scale in predicting its many-body behaviors. As we show in the Appendix, the polaron system in momentum space with four-fermion interactions, the modified level distribution (from GUE to another one between GUE and GSE) can be described and explained in terms of the additional momentum q -dependent Gaussian wave functions Φ_{ik} and Φ_{jl} .

6 Appendix: SYK-type polaron behavior in terms of momentum space representation

Similar to Eq.(1), we can illustrating this model in momentum space as, (for fermions with scaling dimension 1/4),

$$H_{SYK} = \sum_{i<j;k<l} \Phi_{-q}^{ij} \Phi_q^{kl} c_i^\dagger c_k^\dagger c_l c_j = \sum_{i<j;k<l} J_{ik;jl} \Phi_{-q} \Phi_q c_i^\dagger c_k^\dagger c_l c_j, \tag{46}$$

where $i, j, k, l = 1 \cdots N$. J_{ijkl} is an antisymmetry tensor which follows a Gaussian distribution with zero mean. To adding the DOF related to scattering momenta, we introduce the following s -wave operators which can expressed in terms of the eigenfunctions of SYK Hamiltonian

$$\begin{aligned}\Phi_{-q}^{ij} &= \Phi_{-q} c_i^\dagger c_j, \\ \Phi_q^{kl} &= \Phi_q c_k^\dagger c_l.\end{aligned}\tag{47}$$

Here the Gaussian variables (i, k) and (j, l) with, respectively, the scattering momenta $-q$ and q , correspond to the i and j in Eq.(1), and the polaronic momentum wavefunction $\phi_{-q}\phi_q$ related to the potential difference-DOF in Eq.(1). The coupling satisfies

$$\delta_{ik}\delta_{jl}J_{i<j;k<l} = - \sum_q^{\Lambda_q} \Phi_{ij}^{-q} g_q \Phi_{kl}^q.\tag{48}$$

We restrict that, projecting to momentum space, the flavor number of the third DOF, which is the $O(M) \sim \frac{N^2}{4}$ in Eq.(1). As the variance $\sigma_\Delta^2 \sim \frac{N^2}{4} = \frac{g_{(3)}^2}{3N^2} \frac{3N^2}{2} = \frac{g_{(3)}^2}{2}$, the inverse momentum cutoff reads $\Lambda_q^{-1} = \frac{2J}{N^2}$, where $g_{(3)}^2 = \frac{N^2}{2}$ is the constant parameter as stated in Sec.3, and J^2 is the corresponding coupling in momentum space but also in dimensions of energy. This result is in consistent with the final variance in Eq.(57).

As we stated in above, the calculations related to the polaron dynamics usually requires momentum cutoff Λ_q . The polaron coupling reads (with E_b the binding energy and W the bandwidth)

$$g_q^{-1} = - \sum_{kp}^{\Lambda} \frac{1}{E_b + \varepsilon_p + \varepsilon_k + W},\tag{49}$$

which vanishes in $\Lambda \rightarrow \infty$ limit. Similarly, in two space dimension, the polaron corresponds to the pole $q = ia^{-1}$ where a is the scattering length (or scattering amplitude), which proportional to the polaronic coupling strength, and the strongest polaronic coupling realized at $q \sim a^{-1}$ while the weakest coupling realized at $qa \ll 1$. This is a special property of polaron formation and is important during the following analysis. Now we know that g_q is inversely proportional to the value of polaronic exchanging momentum q , then by further remove the q -dependence of polaronic coupling

$$g^{-1} = - \sum_q^{\Lambda_q} \sum_{kp}^{\Lambda} \frac{1}{E_b + \varepsilon_{p-q} + \varepsilon_{k+q} + W},\tag{50}$$

the integral in Eq.(50) is vanishingly small when $\Lambda_q \rightarrow \infty$. Note that in the following we may still use g_q to denote the polaronic coupling to distinct it from the SYK one.

In opposite limit, when $\Lambda_q \rightarrow 0$, both the couplings J_{ijkl} and g_q become very strong (thus enters the SYK regime). Similar to the disorder effect from temperature (which is lower than the coherence scale but higher than other low energy cutoff) to Fermi liquid, the fermion frequency can be treated as a disorder to non-Fermi liquid SYK physics, (the pure SYK regime can be realized in $\omega, \omega_c \rightarrow 0$ limit and extended to zero temperature) thus we can write the essential range of parameter to realizes SYK physics,

$$\Lambda_q^{-1} \sim \frac{g_q}{\omega} v_F \gg N,\tag{51}$$

this is one of the most important result of this paper which relates the polaron physics to the SYK physics, and in the mean time, it is surely important to keep $N \gg U \gg \omega \gg \omega_c \gg U/N$. Here the $\omega \sim v_F q$ plays the role of disorder in frequency space. Note that here vanishingly small cutoff in momentum space Λ_q corresponds to vanishing spacial disorder Λ_r which is the lattice

spacing in two-dimensional lattice in real space[14]. That is, in the presence of short range interaction, by reducing the distance between two lattice sites (and thus enlarging the size of hole), the size number as well as the coupling is increased. Thus in this case the polaron term becomes asymptotically Gaussian distributed due to the virtue of the central limit theorem.

In the $\Lambda_q = 0$ limit (SYK), the Hamiltonian can be rewritten in the exact form of SYK $_{q=2}$ mode.

$$\begin{aligned} H_p &= g_q \sum_{ik} \sum_{\sigma, \sigma'} \Phi_i c_i^\dagger c_i \Phi_k c_{k\sigma'}^\dagger c_k \\ &\equiv g_q \sum_{ik} \sum_{\sigma, \sigma'} b_i b_{k\sigma'}, \end{aligned} \quad (52)$$

where $b_i = \Phi_i c_i^\dagger c_i$ and $[b_i, H_p] = 0$. After disorder average in Gaussian unitary ensemble (GUE), for Gaussian variable $\Phi_{ik} \Phi_{jl}$, we have

$$\overline{\Phi_{ik} \Phi_{jl}} = 0, \quad (53)$$

and the replication process reads

$$g_q \Phi_{il} \Phi_{jk} \mathcal{O}_{il,jk} \rightarrow -\frac{J^2 \delta_{ij} \delta_{jk} 2\mathcal{O}_{il,jk}^\dagger \mathcal{O}_{il,jk}}{16N^2} = -\frac{J^2 \delta_{ij} \delta_{jk} \mathcal{O}_{il,jk}^\dagger \mathcal{O}_{il,jk}}{8N^2}. \quad (54)$$

Note that before replication, the number of observable \mathcal{O} should equals to the number of Gaussian variables, which is one in the above formula. While in the finite but small Λ_q case

$$H_p = g_q \sum_{il;jk} \sum_{\sigma, \sigma'} \Phi_{il}^{-q} \Phi_{jk}^q c_i^\dagger c_i c_{j\sigma'}^\dagger c_{k\sigma'}, \quad (55)$$

where we have

$$\begin{aligned} g_q \Phi_{il}^{-q} \Phi_{jk}^q \mathcal{O}_{ik}^\dagger \mathcal{O}_{lj} 2\mathcal{O}_q^\dagger \mathcal{O}_q &\rightarrow \frac{J_{il;jk}^2 \delta_{il} \delta_{jk} \Lambda_q^2 4\mathcal{O}_{ik} \mathcal{O}_{ik}^\dagger \mathcal{O}_{lj}^\dagger \mathcal{O}_{lj} (2\mathcal{O}_q^\dagger \mathcal{O}_q)^2}{16N^2} \\ &= \frac{J_{il;jk}^2 \delta_{il} \delta_{jk} \Lambda_q^2 \mathcal{O}_{ik} \mathcal{O}_{ik}^\dagger \mathcal{O}_{lj}^\dagger \mathcal{O}_{lj} (\mathcal{O}_q^\dagger \mathcal{O}_q)^2}{N^2}. \end{aligned} \quad (56)$$

Note that each operator \mathcal{O} must contains q completely independent (uncorrelated) indices, and before replication, the indices of each operator \mathcal{O} must not be completely the same. For example, in the finite (although small) Λ_q case, i (l) is completely independent of k (j), but index ik is not completely uncorrelated with lj because mapping to their momentum space they have $i - l = k - j$ due to the fixed polaronic momentum q , in other word, the mechanism that transforms i to l is the same with that to transform k to j , thus ik can continuously mapped to lj .

In case of finite (but small) Λ_q with approximately uncorrelated random Gaussian variables Φ_{ik} and Φ_{jl} ($\overline{\Phi_{ik}} = \overline{\Phi_{jl}} = 0$, $g_q \overline{\Phi_{ik}^2} = g_q \overline{\Phi_{jl}^2} = \frac{J}{2N} 2\Lambda_q = \frac{J}{N} \Lambda_q$), we can perform the disorder averages over fermion indices and the q in the same time, which leads to the following mean value and variance of Chi-square random variable $g_q \Phi_{il}^{-q} \Phi_{jk}^q$

$$\begin{aligned} \overline{g_q \Phi_{il}^{-q} \Phi_{jk}^q} &= \overline{g_q \Phi_{il}^{-q} \Phi_{jk}^q} = 0, \\ \overline{(g_q \Phi_{il}^{-q} \Phi_{jk}^q)^2} &= g_q^2 \overline{(\Phi_{il}^{-q})^2 (\Phi_{jk}^q)^2} \\ &= \frac{J^2 4\Lambda_q^2}{4N^2} \\ &= \frac{J^2 \Lambda_q^2}{N^2}. \end{aligned} \quad (57)$$

The second line is valid because $(\Phi_{il}^{-q}\Phi_{jk}^q)^2 = (\Phi_{il}^{-q})^2(\Phi_{jk}^q)^2$ when Φ_{il}^{-q} is independent of Φ_{jk}^q , and we assume the variance of $\Phi^{-q}\Phi^q$ is zero throughout this paper. Note that this is only valid in the case that the disorder average over q fermion indices are done separately, i.e., the degree of freedom of q will not affect the correlation between Φ_{il} and Φ_{jk} , and vice versa. Besides, q must be integrated in the same dimension of N , i.e., one dimension (which is the case we focus on in this paper), and thus Λ_q is in the same scale with N . If the q -integral is carried out in d -space dimension, then the above result becomes

$$\overline{(g_q^2\Phi_{il}^{-q}\Phi_{jk}^q)^2} = \frac{J^2\Lambda_q^{2d}}{N^2}. \quad (58)$$

because the sample number of q is related to spacial dimension d .

Next we take the spin degree of freedom into account. To understand the effects of perturbation brought by finite small q (where the polaronic coupling is still approximately viewed as a constant), we use the SU(2) basis to deal with the degree of freedom of spin (i.e., of impurity and majority particles), $\Phi_{\sigma=\pm} = \frac{1}{\sqrt{2}}(\Phi_1 \pm i\Phi_2)$, Then we have

$$\begin{aligned} & g_q \sum_{\sigma,\sigma'=\pm} \sum_{il;jk} \sum_q^{\Lambda_q} \Phi_{il}^{-q}\Phi_{jk}^q \\ &= g_q \sum_q^{\Lambda_q} \sum_{il;jk} \left(\frac{1}{2}(\Phi_{il1}^{-q} + i\Phi_{il2}^{-q})(\Phi_{jk1}^q - i\Phi_{jk2}^q) - \frac{1}{2}(\Phi_{il1}^{-q} - i\Phi_{il2}^{-q})(\Phi_{jk1}^q + i\Phi_{jk2}^q) \right) \\ &= g_q \sum_q^{\Lambda_q} \sum_{il;jk} (i\Phi_{il2}^{-q}\Phi_{jk1}^q - i\Phi_{il1}^{-q}\Phi_{jk2}^q). \end{aligned} \quad (59)$$

And we obtain the variance

$$\begin{aligned} g_q\Phi_{il1}^{-q}\Phi_{jk1}^q 2\mathcal{O}_{il}^\dagger\mathcal{O}_{il} &= g_q\Phi_{il2}^{-q}\Phi_{jk2}^q 2\mathcal{O}_{il}^\dagger\mathcal{O}_{il} = \frac{J}{4N}\delta_{il,jk}2\Lambda_q 2\mathcal{O}_{il}^\dagger\mathcal{O}_{il}, \\ \overline{g_q\Phi_{il1}^{-q}\Phi_{jk1}^q} &= \overline{g_q\Phi_{il2}^{-q}\Phi_{jk2}^q} = \frac{J\Lambda_q}{N}\delta_{il,jk}, \\ \overline{\Phi_{il1}^{-q}\Phi_{jk2}^q} &= 0, \end{aligned} \quad (60)$$

where $J > 0$. Thus Φ_{il1}^{-q} is orthogonal with Φ_{jk2}^q (as long as the Φ_{ik} is approximately treated as independent of Φ_{jl} in the small Λ_q limit (e.g., the SYK limit)). Combined with Eq.(57), we know the variance $\text{Var}(g_q\Phi_{il1}^{-q}\Phi_{il1}^q) = \text{Var}(g_q\Phi_{jk2}^{-q}\Phi_{jk2}^q) = 0$, which is different to the result of next section.

In the small (but finite) Λ_q limit, according to semicircle law, the spectral function of single fermion reads

$$\rho(\varepsilon) = \frac{1}{\pi J} \sqrt{1 - \frac{\varepsilon^2}{4J^2}} = \frac{1}{2\pi J^2} \sqrt{4J^2 - \varepsilon^2}, \quad (61)$$

with

$$J^2 = \overline{(g_q\Phi_{1il}^{-q}\Phi_{2jk}^q)^2} \frac{N^2}{\Lambda_q^2}. \quad (62)$$

The mean value of eigenvalues is thus

$$\left| \int_{\varepsilon < 0} d\varepsilon \varepsilon \rho(\varepsilon) \right| \approx \frac{4J}{3\pi}. \quad (63)$$

Then we obtain that the matrices $g_q\Phi_{1il}^{-q}\Phi_{2jk}^q$ and Φ_{1il}^{-q} and Φ_{2jk}^q are $\frac{N^2}{\Lambda_q} \times \frac{N^2}{\Lambda_q}$ (a $\infty \times \infty$) matrix, and now these matrices are automatically diagonalized. In such a configuration constructed by

us, $g_q \Phi_{1il}^{-q} \Phi_{2jk}^q$ can not be simply viewed as a product of matrices $g_q \Phi_{il} \Phi_{jk}$ and $g_q \Phi^{-q} \Phi^q$, since $g_q \Phi_{il} \Phi_{jk}$ is a $N^2 \times N^2$ matrix while $g_q \Phi^{-q} \Phi^q$ is a $\Lambda_q^{-1} \times \Lambda_q^{-1}$ diagonal matrix ($q \neq 0$ here). Instead, it requires mapping $il(jk) \rightarrow \frac{il(jk)}{\sqrt{\Lambda_q}}$ and $q \rightarrow q \frac{1}{N^2}$ (to realizes $\delta \Lambda'_q = \Lambda_q'^2 = \Lambda_q^2 \frac{1}{N^2}$). This is the SYK phase with gapless SYK mode, and it requires $\Lambda_q^{-1} \gg N$.

6.1 Removable the correlation between Φ_{ik} and Φ_{jl} by summing over q

The SYK phase can be gapped out due to the broken symmetry by finite eigenvalue of $\overline{(g_q \Phi_{1ik} \Phi_{2jl})^2}$ (or $\overline{(g_q \Phi_{il} \Phi_{jk})^2}$). To understand this, it is more convenient to use another configuration, where we carry out the summation over q first in Eq.(34), instead of carrying out the disorder averages over $ijkl$ and q in the same time. Then the disorder average over fermion indices i, j, k, l simply results in

$$\overline{(g_q \Phi_{1ik} \Phi_{2jl})^2} = \frac{J_{il;jk}^2}{4N^2}, \quad (64)$$

which can be calculated as

$$\begin{aligned} \overline{(g_q \Phi_{1ik} \Phi_{2jl})^2} &= \overline{\left(\sum_q^{\Lambda_q^{-1}} g_q \Phi_{1il}^{-q} \Phi_{1jk}^q \right)^2} \\ &= \overline{(g_q \Phi_{1il}^{-\delta \Lambda_q} \Phi_{1jk}^{\delta \Lambda_q} + g_q \Phi_{1il}^{-2\delta \Lambda_q} \Phi_{1jk}^{2\delta \Lambda_q} + \dots)^2} \\ &= \overline{(g_q \Phi_{1il}^{-\delta \Lambda_q} \Phi_{1jk}^{\delta \Lambda_q})^2 + (g_q \Phi_{1il}^{-2\delta \Lambda_q} \Phi_{1jk}^{2\delta \Lambda_q})^2 + \dots} \\ &= \frac{J^2}{4N^2} \sum_q (\Phi^{-q} \Phi^q)^2 \\ &= \frac{J^2 4\Lambda_q}{4N^2} \\ &= \frac{J^2 \Lambda_q}{N^2}, \end{aligned} \quad (65)$$

i.e., $J_{il;jk}^2 = 4\Lambda_q J_{il;jk}^2$. The third line is due to the fact about variance of Gaussian variables: $\text{Var}(A+B) = \text{Var} A + \text{Var} B$ where A and B are independent with each other. The fourth line is because

$$\begin{aligned} \text{Var}(\Phi^q) &= \overline{(\Phi^q)^2} - (\overline{\Phi^q})^2 = 2\Lambda_q - 0 = 2\Lambda_q, \\ \text{Var}(\Phi^{-q} \Phi^q) &= \overline{(\Phi^{-q} \Phi^q)^2} - (\overline{\Phi^{-q} \Phi^q})^2 = 4\Lambda_q^2 - (2\Lambda_q)^2 = 0, \\ \sum_q \Phi^{-q} \Phi^q &= \overline{\Phi^{-q} \Phi^q} \Lambda_q^{-1} = 2, \\ \sum_q (\Phi^{-q} \Phi^q)^2 &= \overline{(\Phi^{-q} \Phi^q)^2} \Lambda_q^{-1} = 4\Lambda_q, \end{aligned} \quad (66)$$

where $\Phi^{-q} \Phi^q$ is obviously not a Gaussian variable (just like the $\Phi_{ik} \Phi_{jl}$ except in the SYK limit), and $\overline{\Phi^{-q} \Phi^q} = \overline{(\Phi^q)^2} \neq \overline{\Phi^{-q}} \overline{\Phi^q} = 0$ because it is impossible to make Φ^{-q} and Φ^q orthogonal to each other due to the connection between them $q = -(-q)$. That is to say, although Φ^{-q} and Φ^q are Gaussian variables with zero mean $\overline{\Phi^{-q}} = \overline{\Phi^q} = 0$, their product $\Phi^{-q} \Phi^q$ is not a Gaussian variable and do not have zero mean. This is different to the variance of Chi-square variable $\Phi_{1ik} \Phi_{2jl}$ which is finite due to the zero mean $\overline{\Phi_{1ik} \Phi_{2jl}} = \overline{\Phi_{1ik}} \overline{\Phi_{2jl}} = 0$, by treating them to be approximately mutually orthogonal (i.e., Φ_{ik} approximately independent with Φ_{jl}). Here we

note that following relations in new configuration

$$\begin{aligned}
\sqrt{|g_q|}\Phi_{1ik} &= \sqrt{g_q}\Phi_{2jl} = 0, \\
\text{Var}(\sqrt{|g_q|}\Phi_{1ik}) &= \overline{g_q\Phi_{1ik}^2} = \frac{J}{2N}2 = \frac{J}{N}, \\
\text{Var}(\sqrt{|g_q|}\Phi_{2jl}) &= \overline{g_q\Phi_{2jl}^2} = \frac{J}{2N}2 = \frac{J}{N}, \\
\text{Var}(g_q\Phi_{1ik}\Phi_{1jk}) &= \overline{(g_q\Phi_{1ik}\Phi_{1jk})^2} - \overline{g_q\Phi_{1ik}\Phi_{1jk}}^2 \\
&= \frac{J^2}{4N^2}4\Lambda_q\delta_{il,jk} - \left(\frac{J}{2N}2\right)^2\delta_{il,jk} \\
&= \frac{J^2}{N^2}(\Lambda_q - 1)\delta_{il,jk}, \\
\overline{g_q\Phi_{1ik}\Phi_{2jl}} &= 0.
\end{aligned} \tag{67}$$

Under this configuration, by approximately treating Φ_{1ik} and Φ_{2jl} to be mutually orthogonal, they can be viewed as two vectors, and each of them contains N^2 components, then $(g_q\Phi_{1ik}\Phi_{2jl})$ is a $N^2 \times N^2$ matrix with complex eigenvalues. But note that, away from the $\Lambda_q^{-1} \rightarrow \infty$ limit, this construction fail because exactly speaking, $(g_q\Phi_{1ik}\Phi_{2jl})$ (after summation over q) is a $N \times N \times N = N^3$ matrix (unlike the $N \times N$ SYK $_{q=2}$ or the $N \times N \times N \times N = N^4$ SYK $_{q=4}$) due to the polaron property, i.e., over the fermion indices i, j, k, l , one of them is always identified by the other three, so there are at most three independent indices (degrees of freedom).

A precondition to treat Gaussian variables $i\Phi_{ik}$ and Φ_{jl} mutually orthogonal (independent), is that it must away from the $\Lambda_q^{-1} \rightarrow \infty$ limit, since too small sample number will makes the matrix $g_q\Phi_{-q}\Phi_q$ leaves away from the Gaussian distribution according to central limit theorem, and thus the disorder average over q can not be successively carried out, that is why we instead make the summation over q . Then, the relation $\Lambda_q^{-1} < N^2/2$ ($\Lambda_q > 2/N^2$) indicates the large number of N , which preserves the Gaussian distribution of Φ_{ik} and Φ_{jl} and also makes the disorder average over fermion indices to matrix $g_q\Phi_{il}\Phi_{jk}$ more reliable, despite the indices il and jk are not completely independent but correlated by some certain mechanism before the summation over q .

Then we turning to the matrix

$$g_q\Phi_{il}^{-q}\Phi_{jk}^q = ig_q\Phi_{1il}^{-q}\Phi_{2jk}^q - ig_q\Phi_{2il}^{-q}\Phi_{1jk}^q, \tag{68}$$

which is also a $N^2 \times N^2$ matrix now and is Hermitian (whose eigenvectors and eogenvalues are much more easy to be solved) with all diagonal elements be zero. In this scheme, to make sure $g_q\Phi_{il}\Phi_{jk}$ is a $N^2 \times N^2$ matrix, the disorder average over i, j, k, l must be done after the summation over q . Then to diagonalizing the $N^2 \times N^2$ matrix $g_q\Phi_{il}^{-q}\Phi_{jk}^q$, it requires $\Lambda_q^{-1} < N^2/2$ to make sure all the vectors Φ_{1ik} and Φ_{2jl} are orthogonal with each other within the matrix $g_q\Phi_{il}^{-q}\Phi_{jk}^q$. This is because there at most exists N^2 vectors can orthogonal with each other in N^2 -dimensional space (formed by N^2 -component vectors). In other word, the propose of this is to make sure vectors $\Phi_{il}^{-\delta\Lambda_q}, \Phi_{il}^{-2\delta\Lambda_q}, \dots, \Phi_{ik}^{-\Lambda_q}, \Phi_{jk}^{\delta\Lambda_q}, \Phi_{jk}^{2\delta\Lambda_q}, \dots, \Phi_{jl}^{\Lambda_q}$ are orthogonal to each other.

Then there are $N^2 - 2\Lambda_q^{-1}$ eigenvectors with eigenvalues equal zero (correspond to the ground state), i.e.,

$$\text{Det}[g_q\Phi_{il}^{-q}\Phi_{jk}^q] = 0, \tag{69}$$

and $2\Lambda_q^{-1}$ eigenvectors $\Phi_\sigma = \frac{\Phi_{1ik}^{-q} \pm i\Phi_{2jl}^q}{\sqrt{2}}$ with eigenvalue $\pm \frac{J}{2\Lambda_q^{-1/2}N}$. This can be verified by the rule that for Hermitian matrix the eigenvectors corresponding to different eigenvalues are orthogonal

to each other,

$$\left(\frac{\Phi_1^{-q} + i\Phi_2^q}{\sqrt{2}}\right)^H \cdot \frac{\Phi_1^{-q} - i\Phi_2^q}{\sqrt{2}} = \frac{1}{2}(\Phi_1^{-q} \cdot \Phi_1^{-q} - i\Phi_1^{-q} \cdot \Phi_2^q - i\Phi_1^{-q} \cdot \Phi_2^q - \Phi_2^q \cdot \Phi_2^q) = 0, \quad (70)$$

where $\Phi_1^{-q} \cdot \Phi_2^q = \Phi_1^{-q} \cdot \Phi_2^q = 0$ since they are orthogonal to each other, and superscript H denotes the transpose conjugation (Hermitian conjugate). The result of Eq.(35) is used here.

In the special case of $\Lambda_q^{-1} = N^2/2$, we have, in matrix $g_q\Phi_{il}\Phi_{jk}$, N^2 eigenvectors $\frac{\Phi_1^{-q} \pm i\Phi_2^q}{\sqrt{2}}$ with eigenvalue $\pm \frac{J\Lambda_q}{2\sqrt{2}}$. Then processing the disorder average over $ijkl$ to $g_q\Phi_{\sigma}^{-q}\Phi_{\sigma'}^q$, we have the variance

$$\text{Var}(g_q\Phi_{il}^{-q}\Phi_{jk}^q) = \overline{(g_q\Phi_{il}^{-q}\Phi_{jk}^q)^2} = \overline{(ig_q\Phi_{1il}^{-q}\Phi_{2jk}^q - ig_q\Phi_{2il}^{-q}\Phi_{1jk}^q)^2} = \frac{1}{4} \frac{J^2\Lambda_q}{N^2} = \frac{J^2}{2N^4}, \quad (71)$$

since $\overline{g_q\Phi_{il}^{-q}\Phi_{jk}^q} = 0$. The factor $1/4$ origin from the spin degrees of freedom, and can be verified by the square of eigenvalue λ^2 . Note that here the overline denotes only the disorder average over $ijkl$ index. This result is in consistent with the property of Wigner matrix in GUE

$$\overline{\lambda^2} = \overline{(g_q\Phi_{il}^{-q}\Phi_{jk}^q)^2} = \frac{J^2\Lambda_q}{4N^2} \sim O(N^{-2}), \quad (72)$$

in contrast with that in Gaussian orthogonal ensemble (GOE) which reads $O(N^{-2})(1 + \delta_{il,jk})$. Here λ denote the eigenvalues. The GUE with $\sum \lambda^2 = \frac{J^2\Lambda_q}{4}$ thus corresponds to the SYK non-Fermi liquid case, with continuous distributed peaks in the SYK fermion spectral function, i.e., the level statistics agree with the GUE distribution, and the set of eigenvalues follow an ascending order. In GUE, we also have the relation

$$\langle \mathcal{O}_{il}\mathcal{O}_{jk}^\dagger \rangle = \langle c_i^\dagger c_l c_j^\dagger c_k \rangle = \langle c_i^\dagger c_j^\dagger c_k c_l \rangle = \langle c_i^\dagger c_l \rangle \langle c_j^\dagger c_k \rangle - \langle c_i^\dagger c_k \rangle \langle c_j^\dagger c_l \rangle, \quad (73)$$

at zero temperature. While the GOE corresponds to the case of nonzero pairing order parameter (in which case pair condensation happen at temperature lower than the critical one), and thus admit the anomalous terms. In GOE we have

$$\overline{\lambda^2} = \overline{(g_q\Phi_{il}^{-q}\Phi_{jk}^q)^2} = \frac{J^2\Lambda_q}{4N^2} + \frac{O(\delta_{il,jk})}{N^2}, \quad (74)$$

$$\sum \lambda^2 = \frac{J^2\Lambda_q}{4} + O(\delta_{il,jk}).$$

Thus the GOE has a level repulsion slightly larger than that of GUE in the small level spacing limit during the level statistic. Then if we turn to the many-body localized phase where the thermalization (chaotic) is being suppressed by the stronger disorder, the level statistic follows the Poisson distribution. Since $g\Phi_{il}\Phi_{jk}$ is not a positive-define matrix, the largest eigenvalues splitting happen which corresponds to the discrete spectrum with the level statistics agree with Poisson distribution, i.e., it has the largest eigenvalues $\lambda_{max} = \pm \frac{J\Lambda_q^{1/2}}{2\sqrt{2}}$ and $\frac{N^2-2}{2}$ eigenvalues $\frac{1}{N^2-2}$ and $\frac{N^2-2}{2}$ eigenvalues $\frac{-1}{N^2-2}$. Such a distribution of eigenvalues implies the existence of off-diagonal long range order. When the pair condensation happen, the above relation becomes $\langle c_i^\dagger c_j^\dagger \rangle \langle c_k c_l \rangle$, with the pairing order parameter

$$\Delta_0 = \langle c_k c_l \rangle = \frac{\sum_{kl} \sum_{\sigma\sigma'} c_{\sigma\sigma'} c_k c_l}{2N^{1/2}} \quad (75)$$

where the factor $(2N^{1/2})^{-1}$ origin from the result of disorder average

$$\overline{\Phi_{kl}^2} = \frac{J}{2N} 2 = \frac{J}{N}, \quad (76)$$

$$\overline{\Phi_{kl,\sigma\sigma'}^2} = \frac{J}{4N}.$$

The $N^2 \times N^2$ positive-definite matrix $\langle c_i^\dagger c_j^\dagger \rangle \langle c_k c_l \rangle$ has summation of eigenvalues corresponds to the total number of pairs $\sum \lambda \leq N^2$ and thus $\bar{\lambda} \leq 1$, i.e., $\lambda_{max} = N^2 = \text{Sp} c_i^\dagger c_j^\dagger \langle c_k c_l \rangle \equiv \text{Sp} b_{ij}^\dagger b_{kl}$. We also found that, once the boson-fermion interacting term is taken into account, the maximum eigenvalue reduced to: For $ij \neq kl$, $\lambda_{max} = \text{Sp} b_{ij}^\dagger c^\dagger c b_{kl} \leq \text{Sp}(b_{ij}^\dagger c^\dagger c b_{kl} + c b_{kl} b_{ij}^\dagger c^\dagger) = 0$; For $ij = kl$ ($\Lambda_q = 0$), $\lambda_{max} = \text{Sp} b_{ij}^\dagger c^\dagger c b_{kl} \leq \text{Sp}(b_{ij}^\dagger c^\dagger c b_{kl} + c b_{kl} b_{ij}^\dagger c^\dagger) = \text{Sp} c c^\dagger = \text{Sp}(1 - c^\dagger c) = 1 - \text{Sp} c^\dagger c \leq 1$. The superconductivity emerge when Δ_0 condenses, and in large -N limit, the renormalized Green's function reads

$$G(i\omega)' = \frac{G(i\omega)}{1 + J^2 |\Delta_0^2| G^2(i\omega)}. \quad (77)$$

For a further study about this renormalization effect, see Ref.[27, 24].

In this case, the coupling J within spectral function reads

$$J^2 = 2N^4 \overline{(g_q \Phi_{il}^{-q} \Phi_{jk}^q)^2}, \quad (78)$$

In the $\Lambda_q^{-1} \ll N^2/2$ limit, we can easily know that J is vanishingly small, and the polaronic dynamic then dominates over the SYK dynamic, and the system exhibits Fermi liquid feature. While for $0 \ll \Lambda_q^{-1} < N^2/2$, the system exhibits disordered Fermi liquid feature with sharp Landau quasiparticles, and for positive definite matrix $g_q \Phi_{il} \Phi_{jk}$, since every zero eigenvalue corresponds to a ground state, there are $N^2 - 2\Lambda_q^{-1}$ ground states, and thus the system exhibits degeneracy $2^{N^2 - 2\Lambda_q^{-1}}$. While in the case of $\mu \gg g_q$, the bilinear term as a disorder will gap out the system and lift the degeneracy in ground state, although in some certain systems[22] the near nesting of Fermi surface sheets can prevent the increase of degeneracy by disorder. Here the bilinear term is absent but the finite value of variance $\text{Var}(g_q \Phi_{il} \Phi_{jk})$ with $\Lambda_q^{-1} < N^2/2$ plays its role and drives the SYK non-Fermi liquid state toward the disordered Fermi liquid ground state.

Finally, we conclude that in $\Lambda_q^{-1} \ll N^2/2$ case, although $g_q \Phi_{il} \Phi_{jk}$ is a Hermitian matrix with randomly independent elements and large N , and each of its matrix elements follows the same distribution (distribution of Chi-square variables), the eigenvalue distribution does not follows the semicircle law. This is because, for $\Lambda_q^{-1} < N^2/2$, N^2 -component vectors Φ_1^{-q}, Φ_2^{-q} are mutually orthogonal, i.e., $\Phi_1^q \cdot \Phi_2^{q'} = \Phi_2^q \cdot \Phi_1^{q'} = \Phi_1^q \cdot \Phi_1^{q'} = \Phi_2^q \cdot \Phi_2^{q'} = \delta_{q,q'}$, which leads to large degeneracy in ground state. In this case, the spectral function does not follows the semicircle law, but exhibits three broadened peaks locate on the energies $\varepsilon = 0, \pm \frac{J\Lambda_q^{1/2}}{2N}$, with heights correspond to the numbers of the corresponding eigenvectors.

During the above basis transformation between the original polaron momentum basis and the SYK fermion indices basis, in the $\Lambda_q^{-1} \rightarrow \infty$ limit, only the statistical relations between ϕ_i and ϕ_l or ϕ_j and ϕ_k depends on the value of Λ_q^{-1} , but this dependence on Λ_q^{-1} is also being replaced by number N after the transformation. While the disorder average over q is carried out separately with that of N , which is allowed only under the condition $\Lambda_q^{-1} \gg N^2$, and in this case, the SYK physics cannot be realized if we do the summation over q first which requires $\Lambda_q^{-1} < N^2/2$ to realize SYK physics.

References

- [1] Wu C H. Statistic behaviors of gauge-invariance-dominated 1D chiral current random model[J]. arXiv preprint arXiv:2207.07821, 2022.
- [2] Alexandrov A S. Transition from Fermi liquid to charged Bose liquid: A possible explanation of the isotope shift in high-T c oxides[J]. Physical Review B, 1992, 46(22): 14932.
- [3] Gu Y, Qi X L, Stanford D. Local criticality, diffusion and chaos in generalized Sachdev-Ye-Kitaev models[J]. Journal of High Energy Physics, 2017, 2017(5): 1-37.

- [4] Kohstall C, Zaccanti M, Jag M, et al. Metastability and coherence of repulsive polarons in a strongly interacting Fermi mixture[J]. *Nature*, 2012, 485(7400): 615-618.
- [5] Chowdhury D, Werman Y, Berg E, et al. Translationally invariant non-fermi-liquid metals with critical fermi surfaces: Solvable models[J]. *Physical Review X*, 2018, 8(3): 031024.
- [6] Culcer D. Linear response theory of interacting topological insulators[J]. *Physical Review B*, 2011, 84(23): 235411.
- [7] Sears V F, Svensson E C, Martel P, et al. Neutron-Scattering Determination of the Momentum Distribution and the Condensate Fraction in Liquid He 4[J]. *Physical Review Letters*, 1982, 49(4): 279.
- [8] Schick M. Two-dimensional system of hard-core bosons[J]. *Physical Review A*, 1971, 3(3): 1067.
- [9] Field B, Levinsen J, Parish M M. Fate of the Bose polaron at finite temperature[J]. *Physical Review A*, 2020, 101(1): 013623.
- [10] Christensen R S, Levinsen J, Bruun G M. Quasiparticle properties of a mobile impurity in a Bose-Einstein condensate[J]. *Physical review letters*, 2015, 115(16): 160401.
- [11] Allen S, Tremblay A M S. Nonperturbative approach to the attractive Hubbard model[J]. *Physical Review B*, 2001, 64(7): 075115.
- [12] Sedrakyan T A, Efetov K B. Supersymmetry method for interacting chaotic and disordered systems: The Sachdev-Ye-Kitaev model[J]. *Physical Review B*, 2020, 102(7): 075146.
- [13] Gu Y, Kitaev A, Sachdev S, et al. Notes on the complex Sachdev-Ye-Kitaev model[J]. *Journal of High Energy Physics*, 2020, 2020(2): 1-74.
- [14] Lantagne-Hurtubise é, Li C, Franz M. Family of Sachdev-Ye-Kitaev models motivated by experimental considerations[J]. *Physical Review B*, 2018, 97(23): 235124.
- [15] Pikulin D I, Franz M. Black hole on a chip: proposal for a physical realization of the Sachdev-Ye-Kitaev model in a solid-state system[J]. *Physical Review X*, 2017, 7(3): 031006.
- [16] Sachdev S. Bekenstein-Hawking entropy and strange metals[J]. *Physical Review X*, 2015, 5(4): 041025.
- [17] Buterakos D, Sarma S D. Coupled electron-impurity and electron-phonon systems as trivial non-Fermi liquids[J]. *Physical Review B*, 2019, 100(23): 235149.
- [18] Mahajan R, Barkeshli M, Hartnoll S A. Non-Fermi liquids and the Wiedemann-Franz law[J]. *Physical Review B*, 2013, 88(12): 125107.
- [19] Cha P, Patel A A, Gull E, et al. Slope invariant T-linear resistivity from local self-energy[J]. *Physical Review Research*, 2020, 2(3): 033434.
- [20] Xu C. Gapless bosonic excitation without symmetry breaking: An algebraic spin liquid with soft gravitons[J]. *Physical Review B*, 2006, 74(22): 224433.
- [21] Chen-Huan WU. SYK behaviors generated by on-site Hubbard-type four-fermion on-site random interactions and the related phase transitions. arXiv: 2105.12844.
- [22] Graser S, Maier T A, Hirschfeld P J, et al. Near-degeneracy of several pairing channels in multiorbital models for the Fe pnictides[J]. *New Journal of Physics*, 2009, 11(2): 025016.
- [23] Patel A A, Lawler M J, Kim E A. Coherent superconductivity with a large gap ratio from incoherent metals[J]. *Physical review letters*, 2018, 121(18): 187001.
- [24] Pikulin D I, Franz M. Black hole on a chip: proposal for a physical realization of the Sachdev-Ye-Kitaev model in a solid-state system[J]. *Physical Review X*, 2017, 7(3): 031006.
- [25] Wang Y. Solvable strong-coupling quantum-dot model with a non-Fermi-liquid pairing transition[J]. *Physical review letters*, 2020, 124(1): 017002.
- [26] Chen A, Ilan R, De Juan F, et al. Quantum holography in a graphene flake with an irregular boundary[J]. *Physical review letters*, 2018, 121(3): 036403.

- [27] Patel A A, Sachdev S. Critical strange metal from fluctuating gauge fields in a solvable random model[J]. *Physical Review B*, 2018, 98(12): 125134.
- [28] You Y Z, Ludwig A W W, Xu C. Sachdev-Ye-Kitaev model and thermalization on the boundary of many-body localized fermionic symmetry-protected topological states[J]. *Physical Review B*, 2017, 95(11): 115150.
- [29] Hu X, Pajerowski D M, Zhang D, et al. Freezing of a Disorder Induced Spin Liquid with Strong Quantum Fluctuations[J]. *Physical Review Letters*, 2021, 127(1): 017201.
- [30] Merz F, Chalker J T. Negative scaling dimensions and conformal invariance at the Nishimori point in the J random-bond Ising model[J]. *Physical Review B*, 2002, 66(5): 054413.
- [31] Levy R, Clark B K. Entanglement Entropy Transitions with Random Tensor Networks[J]. arXiv preprint arXiv:2108.02225, 2021.
- [32] Bi Z, Jian C M, You Y Z, et al. Instability of the non-Fermi-liquid state of the Sachdev-Ye-Kitaev model[J]. *Physical Review B*, 2017, 95(20): 205105.
- [33] Skinner B, Ruhman J, Nahum A. Measurement-induced phase transitions in the dynamics of entanglement[J]. *Physical Review X*, 2019, 9(3): 031009.
- [34] Ikegaya S, Kobayashi S, Asano Y. Symmetry conditions of a nodal superconductor for generating robust flat-band Andreev bound states at its dirty surface[J]. *Physical Review B*, 2018, 97(17): 174501.
- [35] Konig E J, Ostrovsky P M, Protopopov I V, et al. Metal-insulator transition in two-dimensional random fermion systems of chiral symmetry classes[J]. *Physical Review B*, 2012, 85(19): 195130.
- [36] Wei C, Sedrakyan T A. Optical lattice platform for the Sachdev-Ye-Kitaev model[J]. *Physical Review A*, 2021, 103(1): 013323.
- [37] Iyoda E, Katsura H, Sagawa T. Effective dimension, level statistics, and integrability of Sachdev-Ye-Kitaev-like models[J]. *Physical Review D*, 2018, 98(8): 086020.
- [38] Tracy C A, Widom H. The distributions of random matrix theory and their applications[J]. *New trends in mathematical physics*, 2009: 753-765.
- [39] Dumitriu I, Edelman A. Matrix models for beta ensembles[J]. *Journal of Mathematical Physics*, 2002, 43(11): 5830-5847.

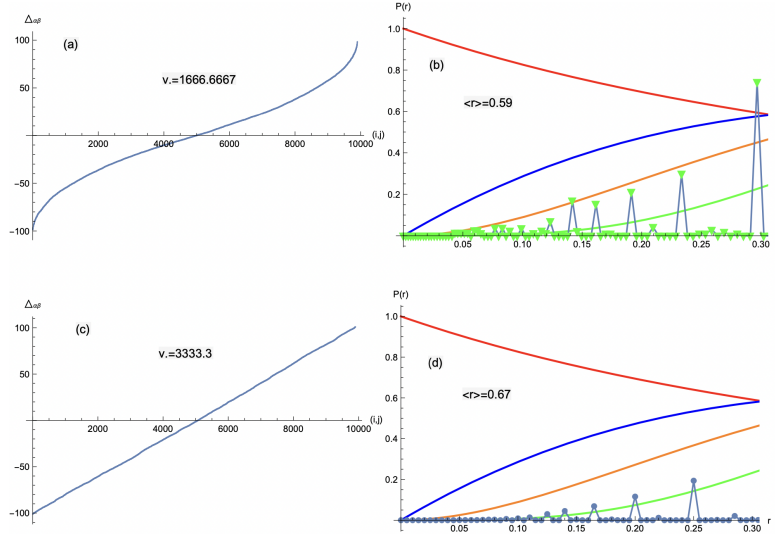


Figure 1: $\Delta_{\alpha\beta}$ -spectrum for four-point interaction (a,b) which follows GUE distribution and two-point interaction (c,d) which follows GSE distribution. In this article we only show the results simulated by setting $N = 100$.

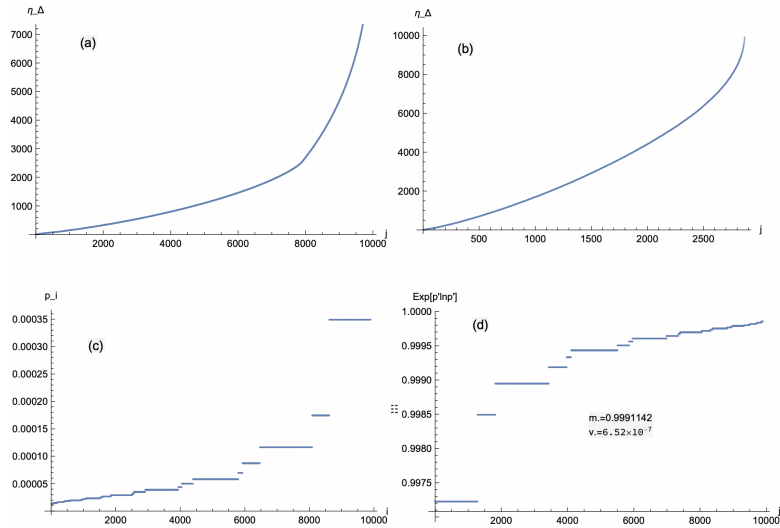


Figure 2: η_{Δ} -spectrum for the unweighted (α, β) -states (a) and the weighted one (b) which corresponds to irreducible group $\{\eta_{\Delta}\}$. For $N = 100$, there will be nearly $O(M) \sim \frac{N^2}{4}$ flavors corresponding to distinct values of η_{Δ} . (c) and (d) show the exact probabilities p_i^j and $(p_i^j)p_i^j$ for each (α, β) -state.

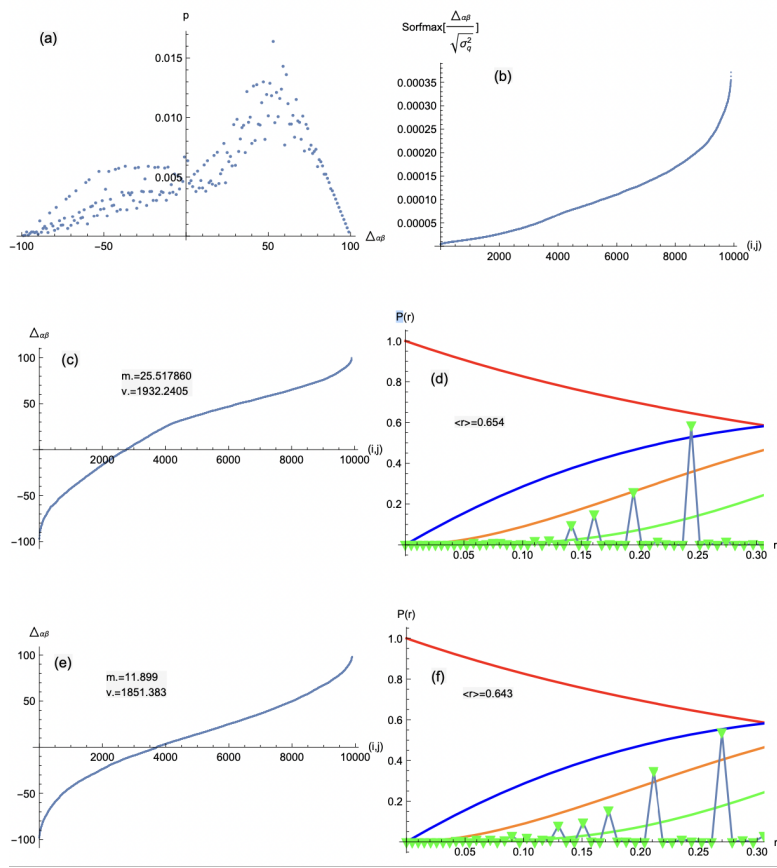


Figure 3: (a) Probability distribution of potential difference $\Delta_{\alpha\beta}$. (b) The softmax-renormalized results (the QT^T matrix) which is available to inner product with the value matrix. (c,d) show the exactly calculated $\Delta_{\alpha\beta}$ -spectrum and the level spacing distribution, while (e,f) show the predicted one using the learnable parameters in self-attention method.

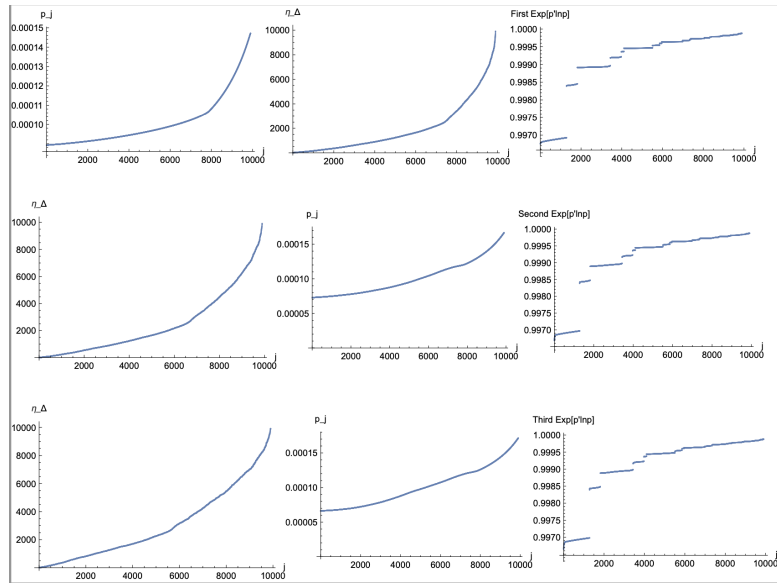


Figure 4: The first, second, and third rows show the three times of learning process using the self-attention method. The learnable parameters are automatically modified after each iteration. The first, second, and third columns are the predicted probability distributions, resulting η_{Δ} -spectrums, and the $p_i^{D_i}$ -spectrum which plays the role of loss function here to better identify the accuracy after each step.